Science
AAAS

NANOMATERIALS

Emergence of hierarchical structural complexities in nanoparticles and their assembly

Chenjie Zeng,[1] Yuxiang Chen,[1] Kristin Kirschbaum,[2] Kelly J. Lambright,[2] Rongchao Jin[1]*

[1]Department of Chemistry, Carnegie Mellon University, Pittsburgh, PA 15213, USA. [2]Department of Chemistry and Biochemistry, University of Toledo, Toledo, OH 43606, USA.

23 DECEMBER 2016 • VOL 354 ISSUE 6319

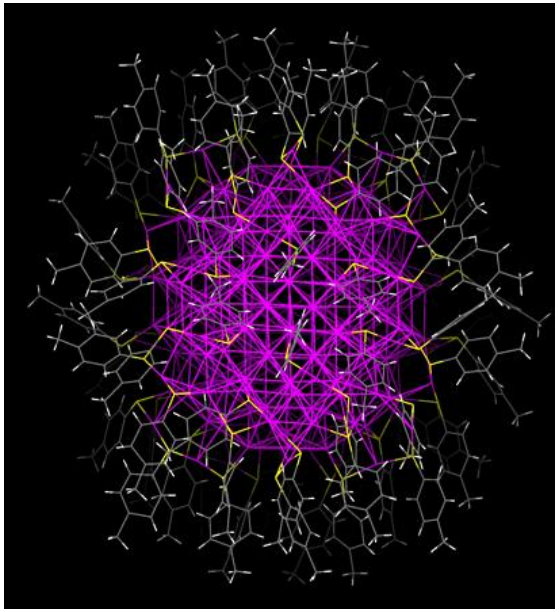

Papri Chakraborty
22.04.2017

Introduction

- Hierarchical self-assembly of nanoparticles(NPs) into complex architectures across different length scales is an important capability in nanotechnology.

- Self-assembly can be driven by entropy dictated maximization of the packing density, as demonstrated in close packing of spheres, binary NPs, rods, and hard polyhedrons. Interparticle interactions, such as the electrostatic attraction, cDNA binding , and patchy NP surfaces, have also been exploited to guide assembly into diverse lattice structures.

- Despite these advances, NP assembly has not achieved the same level of atomic accuracy as in biological systems.

- We now demonstrate that NP-assembled structures can reach the same hierarchy and atomic accuracy as biomolecules at the interparticle and intraparticle levels.

In this paper

It is demonstrated that NP-assembled structures can reach the same hierarchy and atomic accuracy as biomolecules at the interparticle and intraparticle levels.

Through crystallization of uniform 2.2-nm gold NPs bearing p-methylbenzenethiolate (p-MBT) surface ligands [Au_{246}(p-MBT)$_{80}$], the entire self-assembled structures have been resolved at atomic (packing of gold atoms), molecular (packing of surface ligands), and nanoscale (packing of NPs) levels by single crystal x-ray diffraction (SC-XRD).

The protecting ligands self-organize into rotational and parallel patterns on the nanoparticle surface via C-H ···Π interaction, and the symmetry and density of surface patterns dictate directional packing of nanoparticles into crystals with orientational, rotational, and translational orders.

Synthesis and characterization of $Au_{246}(p\text{-}MBT)_{80}$ nanoparticles

Synthesis : Two-step size focussing method

1mM $HAuCl_4$ (dissolved in 5 mL of H_20)
+
1.16 mM of TOAB (dissolved in 10 mL of toluene)

↓ vigorous stirring for 5 min

Clear aqueous phase was removed and
4 mmol of p-MBT added into the toluene phase

↓ vigorous stirring for 30 min

10 mM of $NaBH_4$ (in 5mL of H_2O) was rapidly added
Color turned to black

↓ 10 min

Aqueos phase was removed and toluene phase
was dried by rotary evaporation

↓ Precipitate washed with methanol

$Au_x(p\text{-}MBT)_y$

$Au_x(p\text{-}MBT)_y$
(extracted with CH_2Cl_2)
+
1 mL of p-MBT and 1 mL of toluene

↓ 80 ^oC
Gently stirred
10 hours

Product washed with methanol to remove
Excess thiol and extracted with CH_2Cl_2

↓

$Au_{246}(p\text{-}MBT)_{80}$ (90 % pure)

↓ Further purification by
solvent fractionation with
Toluene/methanol

$Au_{246}(p\text{-}MBT)_{80}$ (pure)

Crystallization
Vapor diffussion of acetonitrile into toluene solution of pure $Au_{246}(p\text{-}MBT)_{80}$ NPs.

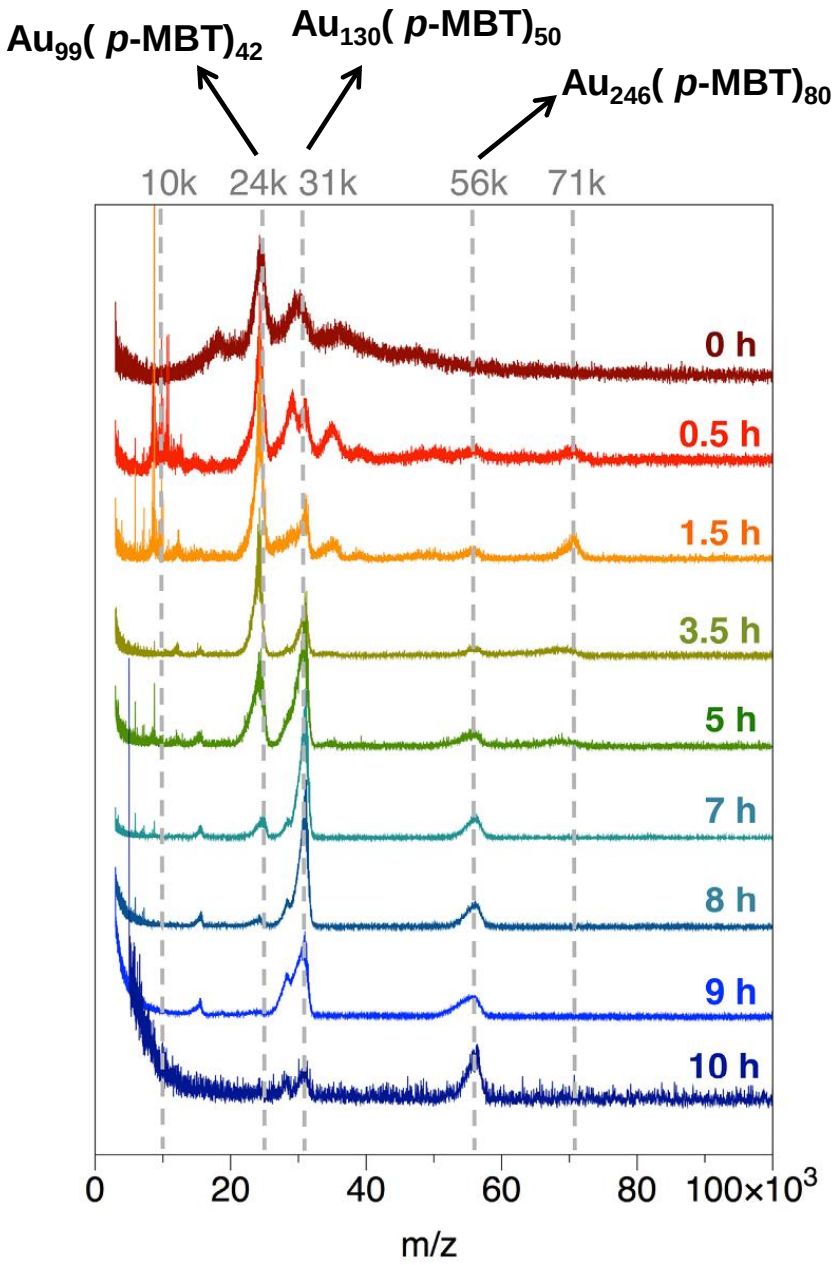

Fig. S1. The size focusing process for the synthesis of Au_{246}(*p*-MBT)$_{80}$ nanoparticles, as monitored by MALDI MS.

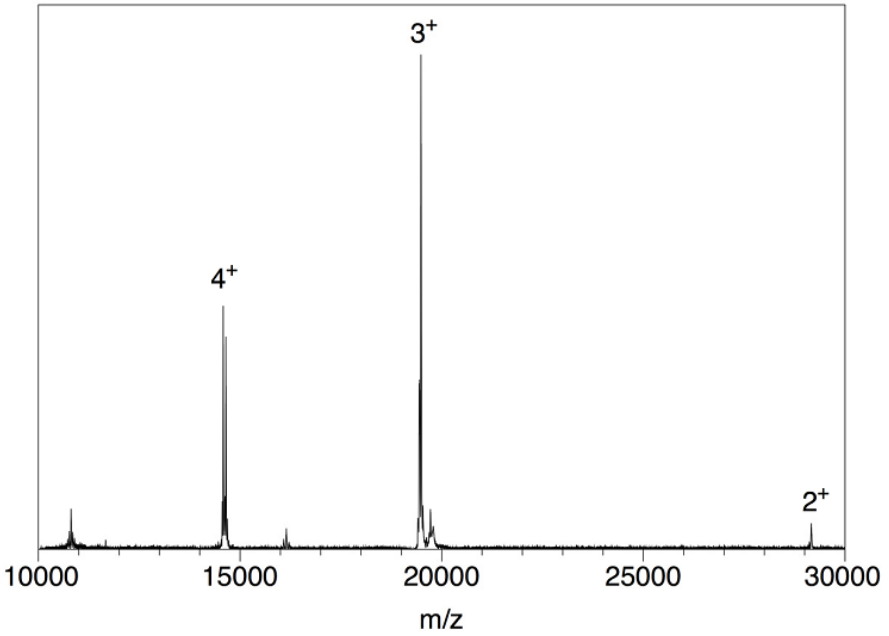

Fig. S2. Electrospray ionization mass spectrometry (ESI MS) of the Au_{246}(*p*-MBT)$_{80}$. The peaks correspond to the 4+, 3+, and 2+ ion sets of Au_{246}(*p*-MBT)$_{80}$ (MW=58,309 g/mol).

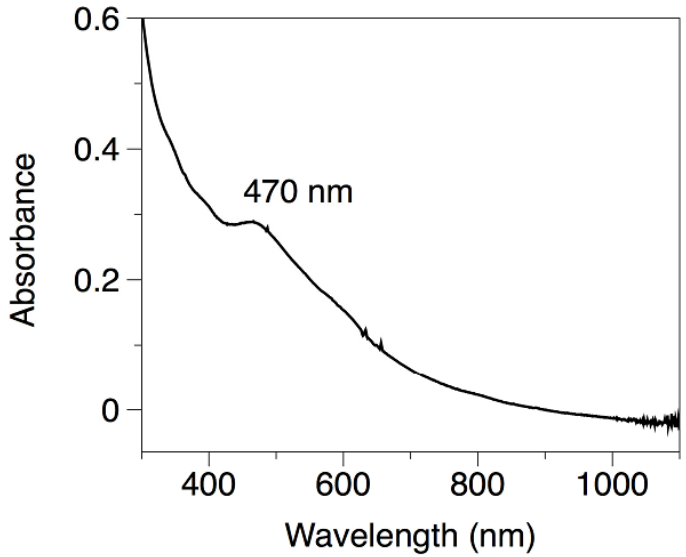

Fig. S3. UV-vis absorption spectrum of the Au_{246}(*p*-MBT)$_{80}$ nanoparticle.

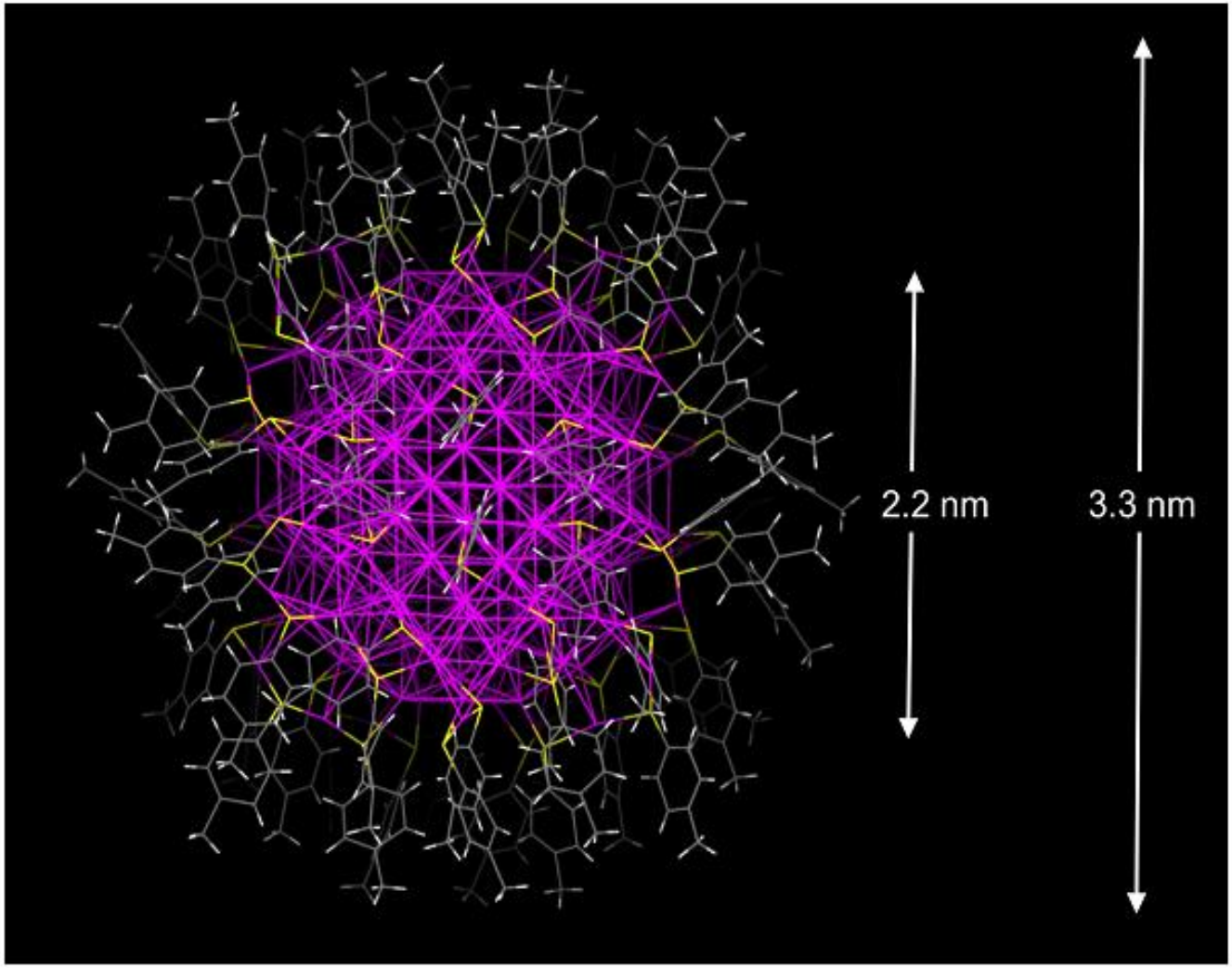

Fig. S4. The overall size and core size of the Au_{246}(*p*-MBT)$_{80}$ nanoparticle.

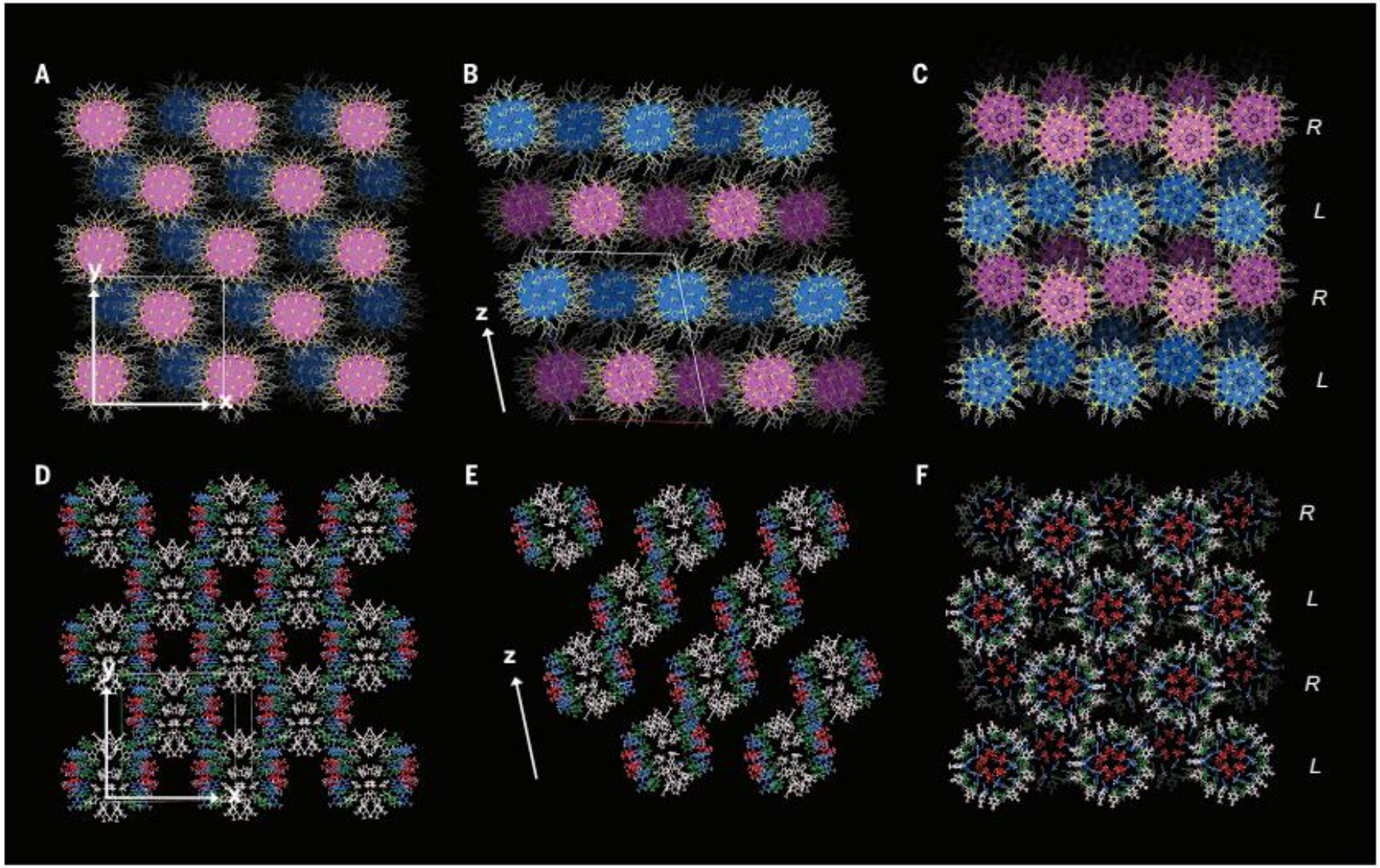

Fig. 1. Packing structure of the derivatized AuNPs in single crystals. (**A** to **C**) View from z direction (A), y direction (B), and x direction (C). Magenta,blue: Au NPs with different chirality; yellow: sulfur; gray: carbon. (**D** to **F**) Alignment of surface ligands among the NPs. Gray: ligands located at the waist of the NP; red, blue, green: ligands located at the poles.

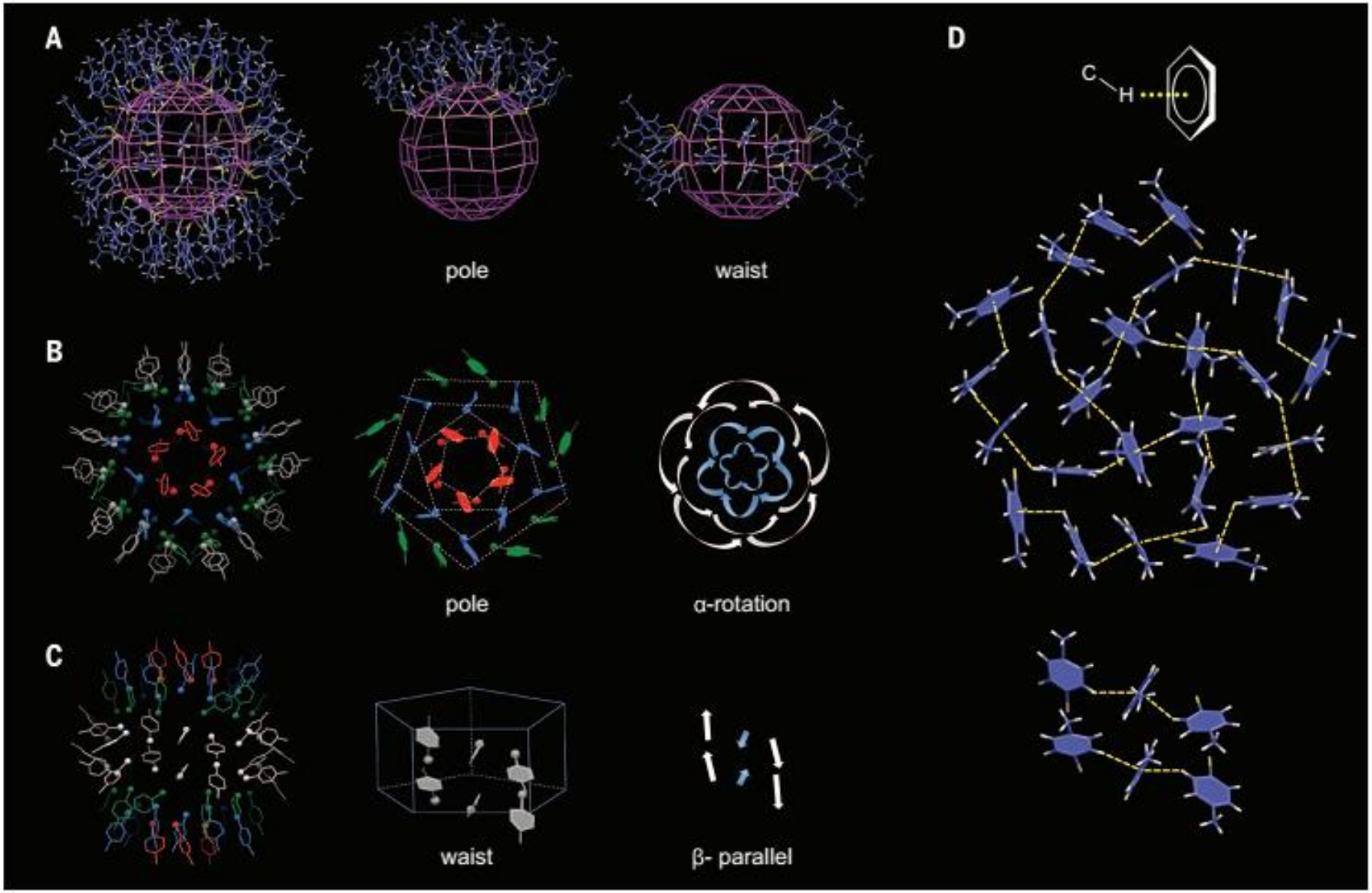

Fig. 2. Self-assembled surface patterns of the ligands on the Au NPs. (**A**) Overall structure of ligands on the surface of NPs. (**B**) Rotational packing of ligands at the pole site of the NP. (**C**) Parallel packing of ligands at the waist of the NP. (**D**) The C-H ···p interactions for stabilizing the large-scale rotational patterns and parallel patterns.

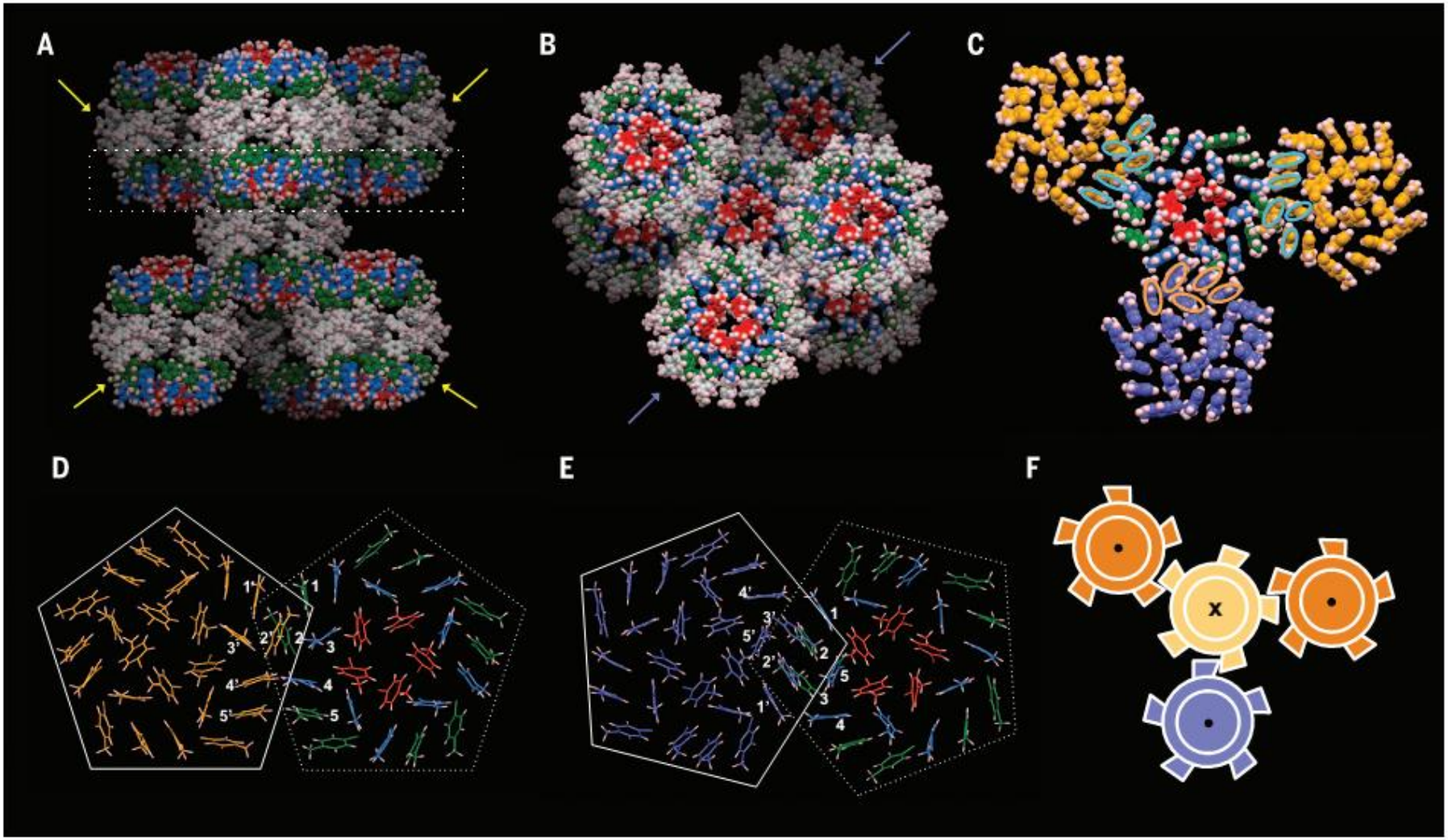

Fig. 3. Interparticle self-assembly dictated by the ligand density and the symmetry of surface patterns. (**A** and **B**) Coordination geometry of NPs in the crystal lattice: side view (**A**) and top view (**B**). (**C**) Contacting environment among the interparticle ligands.The outside pentagons are located at the bottom of the top three nanoparticles in (**A**), and the central pentagon is located at the top of the central nanoparticle. (**D**) Side-by-side stacking of the ligands in the NPs with the same chirality. (**E**) Point-to-point stacking of the ligands in the NPs with opposite chirality. (**F**) Scheme showing the directional packing of NPs achieved through matching the symmetry of surface patterns.

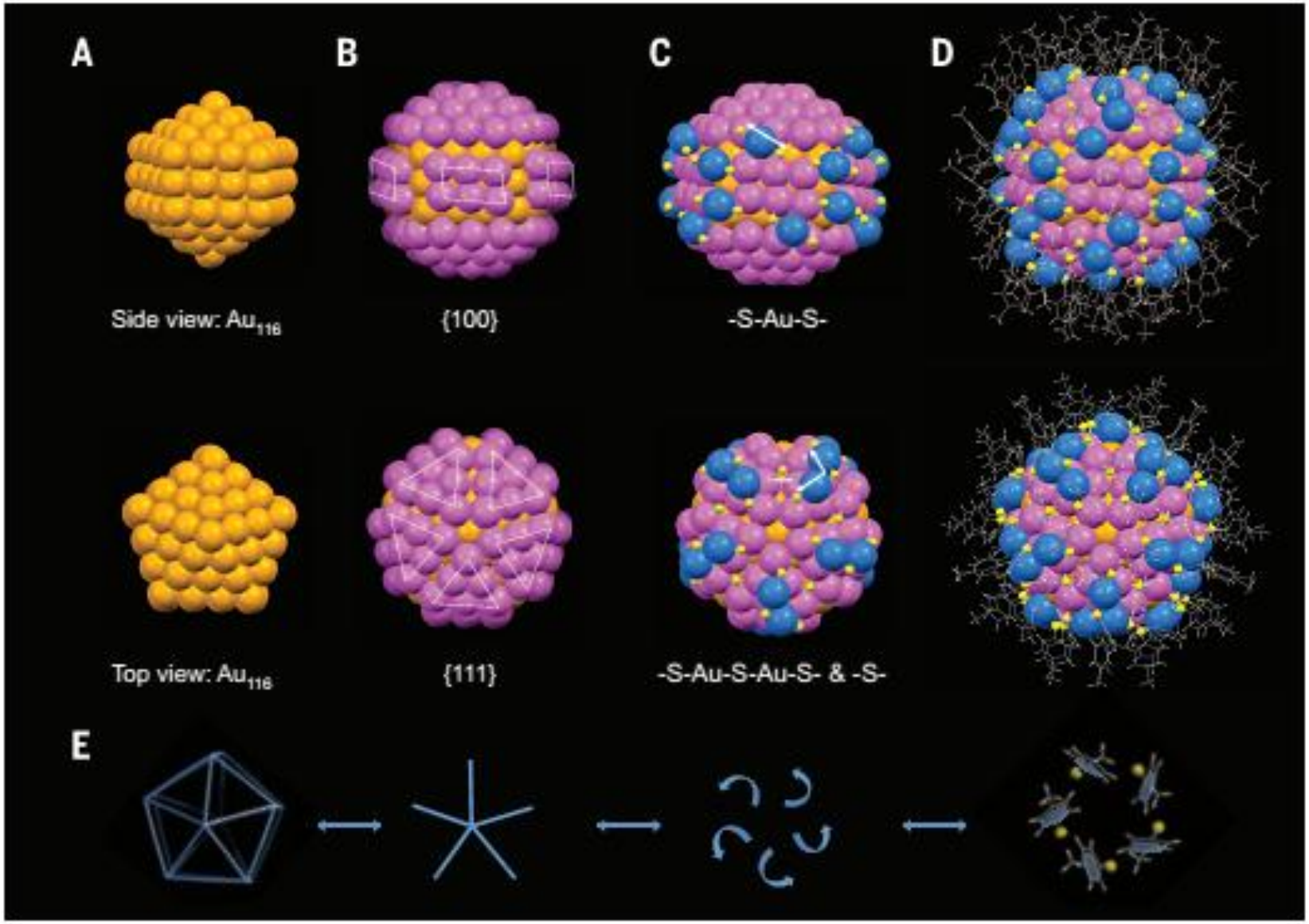

Fig. 4. Intraparticle self-assembly in the Au NP. (**A**) Au116 i-Dh kernel, top: side view; bottom: top view. (**B**) Transition layer structure as colored in magenta. (**C**) Gold-sulfur interfacial structure containing diverse surface protecting motifs. (**D**) Surface carbon layer and overall structure. (**E**) Intraparticle symmetry matching and emergent behavior.

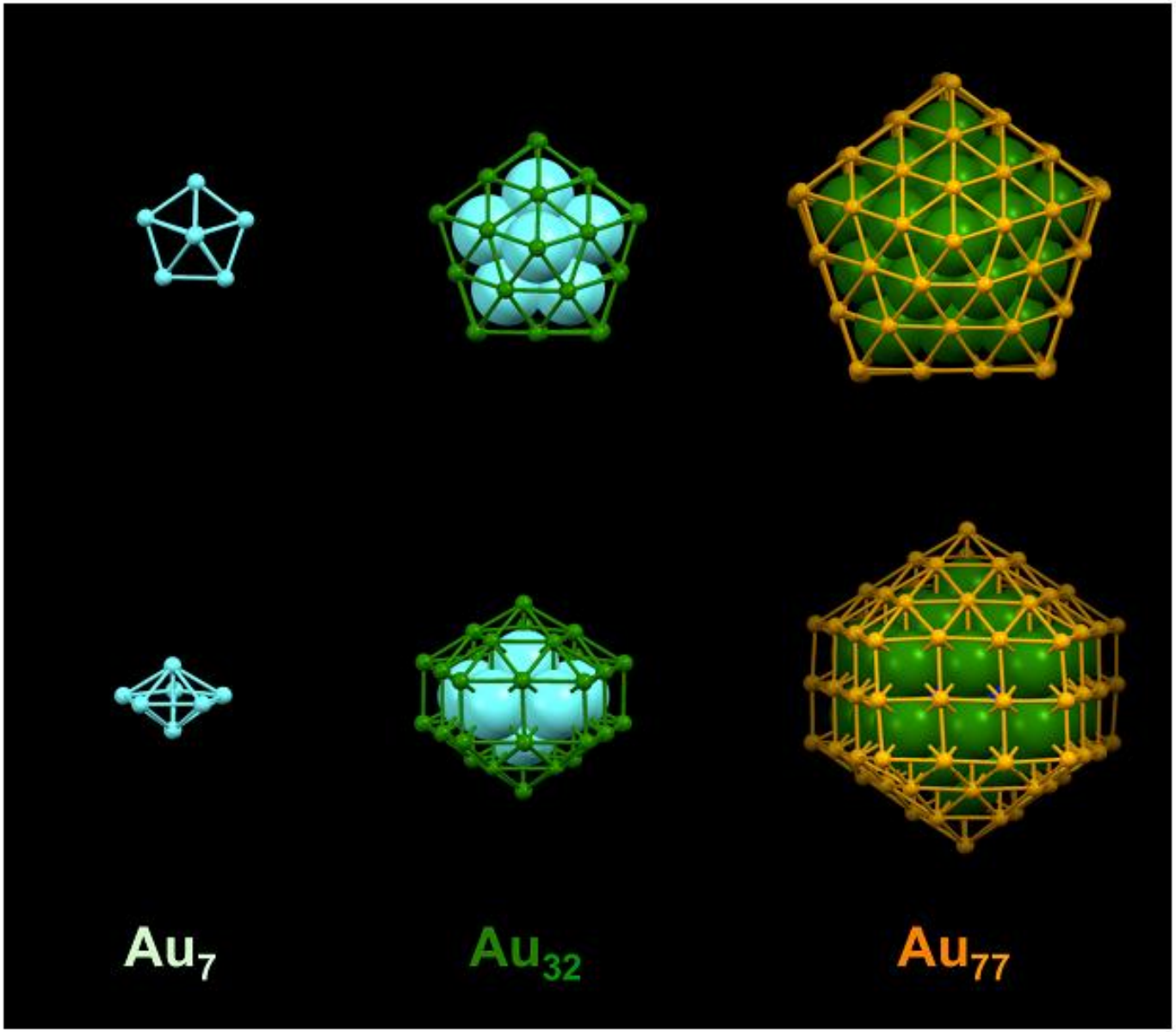

Fig. S8. The three shells (7/32/77 atoms) in the Au_{116} Ino decahedron.

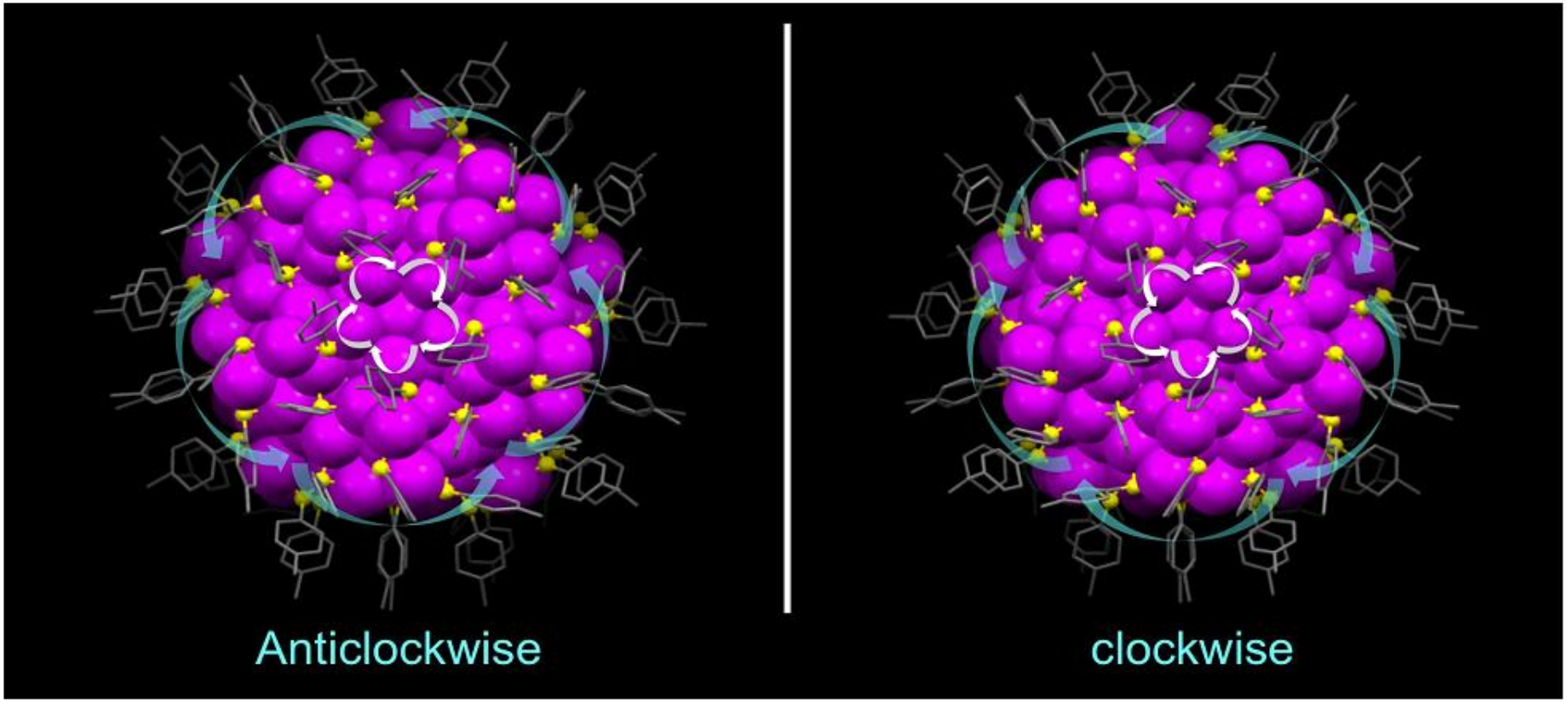

Fig. S10. Chirality in the surface rotational pattern. Left and right nanoparticles corresponds to the two chiral isomers of Au_{246}(*p*-MBT)$_{80}$.

Conclusion

- An intriguing question is whether the packing symmetry of the surface patterns emerged from the core or the core symmetry emerged from the surface.

- Although each part of NP contributes to the overall energy minimization, we deduce that the surface ligands play a pivotal role in guiding the intraparticle assembly, because the gold atoms are less selective when packing into specific structure types such as fcc, decahedron, or icosahedron.

- In addition, the rotational patterns of ligands induce the chirality in the interfacial layer and transitional layer, and packing of gold atoms alone cannot give rise to chirality.

- Also, the larger sphere of the ligands likely has a greater surface energy to minimize, and the structures of Au NPs were highly sensitive to the subtle changes of ligands.